Influence of Pore Gas in Closed-Cell Cellular Structures under Dynamic Loading

Matej Vesenjak[1], Andreas Öchsner[2], Zoran Ren[1]

[1] University of Maribor, Faculty of Mechanical Engineering, Maribor, Slovenia

[2] University of Aveiro, Campus Univ. de Santiago, Aveiro, Portugal

Abstract:

New computational models of closed-cell cellular structures that account for the effects of gas inside the pores are described in this paper. The behaviour of cellular models under uniaxial impact loading and large deformations has been analyzed with the LS-DYNA code. Parametric computational simulations illustrate the effect of pore gas on macroscopic behaviour during deformation regarding the load type. Developed computational models provide insight into material behaviour undergoing large deformations under impact loading and provide grounds for optimization of cellular structure for different application requirements, e.g. crash absorbers.

Keywords:

Cellular structure, closed-cell, impact loading, pore gas influence, LS-DYNA

1 Introduction

Foams and other highly porous materials with a cellular structure have an attractive combination of physical and mechanical properties like high stiffness with regard to low specific weight or high gas permeability combined with high thermal conductivity [7]. Such structures often appear in nature for constructional and functional purposes (i.e. wood, bones). One of the most important and interesting applications of cellular materials can be expected in the automotive industry, where such materials can be used for crash energy absorption.
There exist several homogenization models of cellular structures, which are already implemented in commercial codes. However, these models do not account for the influence of gas inside the closed-cell cellular structure. This paper investigates possibilities of simulating the gas effect and its influence on macroscopic behavior during the deformation for cellular metals under uniaxial impact loading with the LS-DYNA code.

2 Cellular structures

Cellular materials comprise of a wide range of different arrangements and forms (Figure 1) with three typical structures: honeycomb, open-cell structures and closed-cell structures [7]. One of the most important parameters of cellular materials is their specific density (the macroscopic density, divided by the density of the base material). The advantages of cellular materials are low density (light-weight structures), high acoustic isolation and damping, high grade of deformation, high energy absorption, recyclability etc. The cellular metals (usually refered to as metallic foams) have some further advantages like higher strength and heat permeability [2]. Usually they are made of aluminum alloys or polymer materials, with regular or random cell arrangement. Metallic foams have the potential for application in automotive, rail, naval and aerospace industry as heat exchangers, filters, bearings, acoustic dampers, bio-medical implants and elements for energy absorption.

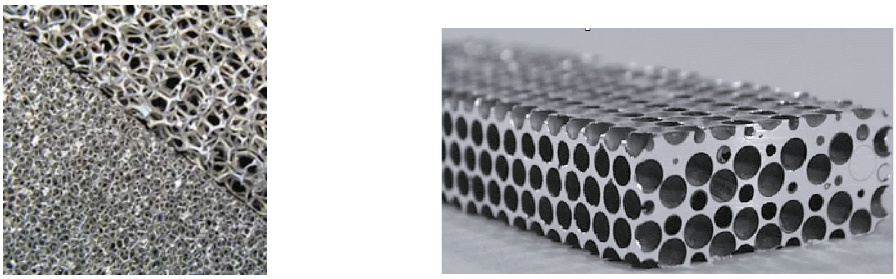

Figure 1: Open-cell (DUOCEL® - left) and closed-cell cellular metals (Körner et. al - right)

Cellular materials have a characteristic stress-strain relationship in compression, which can be divided into four main areas as shown in Figure 2. After initial linear elastic response the cellular materials first experience buckling, plastic deformation and collapse of intercellular walls in the transition zone. Under further loading the mechanisms of buckling and collapse become even more pronounced, which is manifested in large strains at almost constant stress (stress plateau) until the cells completely collapse (densification). At this point the cellular material stiffness increases and consequently converges towards the stiffness of the base material.

During this process the cellular material is able to accumulate the energy through its deformation, which is represented with the area under the strain-stress curve. The accumulated deformation energy is a sum of energy accumulated during elastic deformation and energy absorbed by the plastic deformation. The latter is very important for crash energy absorption and is more pronounced for metal foams than for polymers. It is worth noting that the energy absorption is also strain-rate dependent. The higher the strain-rate, the higher is the capability of deformation energy absorption.
During the manufacturing procedure of closed-cell cellular metals with gas injection (air, CO_2, O_2, Ar) the gas can reach up to 1200 K and 100 MPa according to [2, 12]. After solidification and cooling down, the gas is trapped in the base material. With cells deformation the pore pressure increases, thus, providing increase of structure stiffness up to the point, when the pressure or deformation rises

to the level to cause yielding of the base material. This inavertedly results in collapse of intercellular walls and increase of the material structure porosity [10].

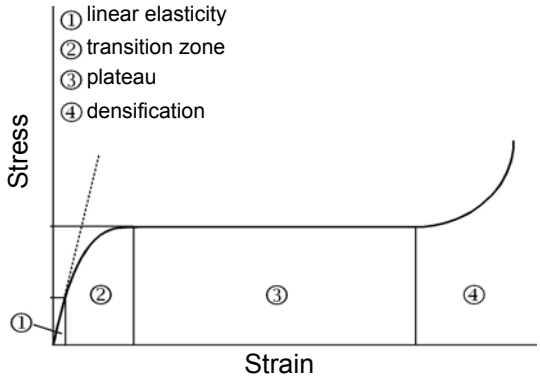

Figure 2: Characteristic stress-strain behavior of cellular materials at compression

Therefore, it is reasonable to investigate the combination of cellular structure with gas filler by determining the gas influence on the macroscopic behavior of cellular metals by means of computational simulations. According to that, parametric computational simulations of the closed-cell cellular structure under impact conditions with different initial pore pressures were performed.

3 Computational analyses

3.1 Numerical model

Complete detailed modeling of cellular materials is usually not possible due to insufficient computer capabilities. For this reason the cellular materials are often modeled by considering a ˝representative volume element˝, which serves for detailed studies of mechanical behavior of a minimum number of unit cells and its mathematical characterization, which is then used as a cellular material constitutive model in consequent computational analyses of complete cellular structure. The minimum number of unit cells must be sufficient to correctly represent macroscopic parameters of cellular material. The precise number depends, on the corresponding cell structure and should be examined separately [11].

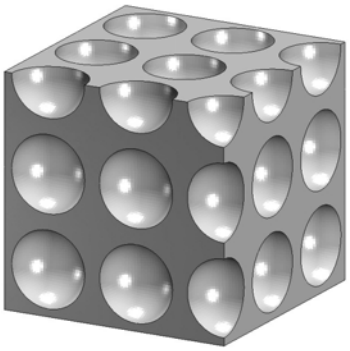

Figure 3: Regular cellular structure

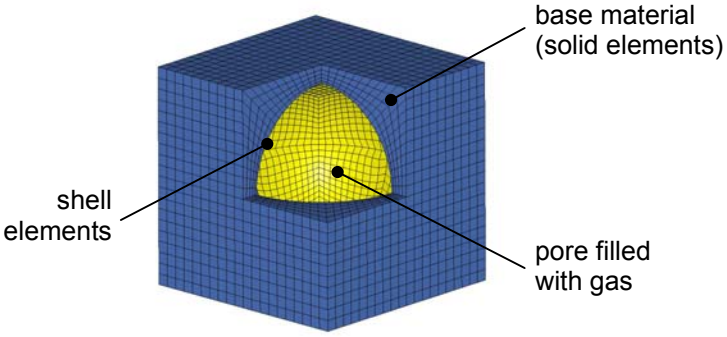

Figure 4: Representative volume element

A regular closed-cell cellular structure was used for the numerical simulation (Figure 3). The representative volume element (Figure 4) was cube-shaped with the edges 1.8 mm in length and a spherical pore with a radius of 0.75 mm. This corresponds to a relative density of 70 %. The base material was meshed with fully integrated 8-noded brick elements.

To consider the gas influence inside the pore a special subroutine (airbag definition) in the LS-DYNA code was used to compute change of pressure, volume and temperature in a closed space [8, 9]. It is presumed that the gas inside the cell has ideal properties (pV/T = const). To define the airbag model, the surface of the pore has to be meshed with shell elements. In order to avoid any additional stiffening of the cellular structure, these shell elements were only 0.01 thick with negligible stiffness.

The nodes of the shell elements were coincident with the inner surface nodes of the base material. The deformation of the structure (change of the pore volume) results in change of gas temperature and internal pore pressure which acts on the structure.
The average size of the elements is 0.05 mm and the whole model consists of 12000 brick elements and 2400 shell elements, together with 85200 degrees of freedom.

3.2 Domain properties

For the base material the aluminum alloy AlCuMg1 was used [11]. The basic material properties are shown in the Table 1 and the stress-strain diagram is shown in the Figure 5.

Table 1: Aluminum alloy properties.

	Density	Elastic modulus	Poisson ratio	Yield stress
AlCuMg1	kg/m^3	GPa	/	GPa
	2700	72.7	0.3	0.3

The strain rate effects were also considered by implementing the Cowper-Symonds constitutive relation [8, 9]

$$\frac{\sigma'}{\sigma} = 1 + \left(\frac{\dot{\varepsilon}}{C} \right)^{1/p}, \tag{1}$$

where σ' is the stress at the strain rate $\dot{\varepsilon}$ and σ is the stress at quasi-static conditions. *C* and *p* are material parameters which characterize the strain rate sensitivity of aluminum alloy [1].

Figure 5 shows the stress-strain diagram of the aluminum alloy at different strain rates.

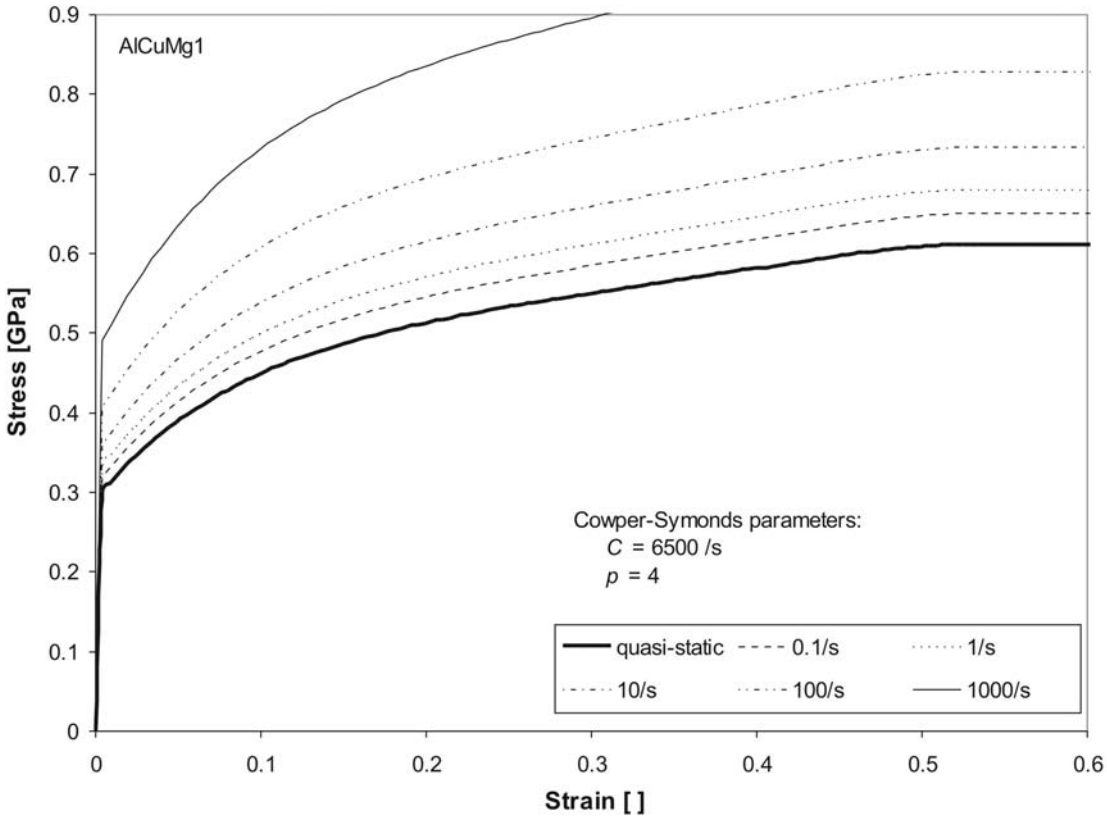

Figure 5: Strain rate effect

The domain inside the pore was filled with the air with the basic properties listed in Table 2.

Table 2: Air properties.

	Density	c_p	c_v	T_0	p_0
Air	kg/m^3	kJ/kg K	kJ/kg K	K	MPa
	1.189	717	1005	293	0.1

3.3 Initial and boundary conditions

The load was displacement controlled and applied to the upper surface of the cell, in order to reach a deformation of 50 % in 5 ms that corresponds to a strain rate of 100 s^{-1} (common for impacts). Two cases were studied: compressive and tensile loading (Figure 6). The lower surface was fixed in the vertical direction. Special periodic boundary conditions were prescribed on side surfaces, where all nodes on a surface have the same displacement in the normal direction to the surface [11, 12]. These boundary conditions were also confirmed with a separate parametric study.

In case of a self-contact at very large deformations the pore surface elements were defined as one contact group, thus effectively accounting for multiple self-contacting regimes during computational analyses. The static and dynamic friction between all parts was set to 0.1 and 0.05, respectively.
The initial pore (gas) pressure was defined with a load curve pressure vs. time. With different initial pressures (0.5, 5, 50 and 100 MPa), its influence on the macroscopic behavior of the cellular material could be studied. Because of the pressure build-up the gas temperature increases and base material is loaded with initial stress (Table 3).

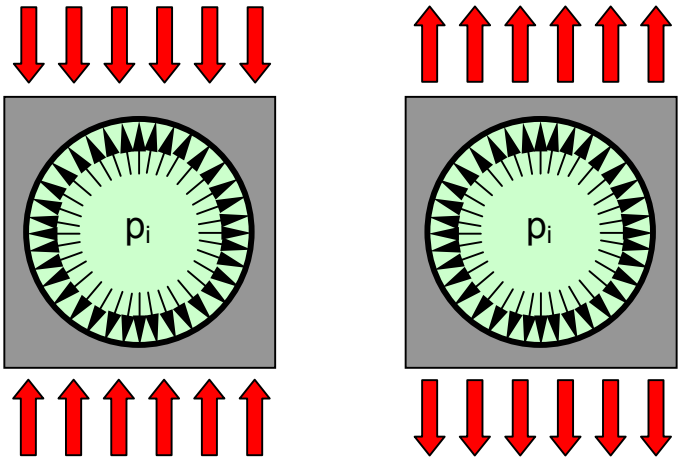

Figure 6: Two loading cases: compression (left) and tension (right)

Table 3: Initial stress in base material due to the pore pressure built-up.

Initial pressure	MPa	0.5	5	50	100
Max $\sigma_{\text{von Mises}}$	MPa	1.4	14	155	230

Dynamic nonlinear explicit finite element code LS-DYNA was used for solving the described model. The analysis time interval was set to 10 ms, with results output required every 0.001 ms. In the first millisecond only the pressure was build up in the pores and after that initialization time the structure was exposed to mechanical load.
The time step for explicit transient dynamic analysis was automatically set by LS-DYNA to 0.1 μs with regard to the lowest resonant frequency of the structure. The analyses run approximately 170 minutes on a PC-cluster consisted of 8 PCs with Intel Pentium IV 3200 MHz processors and 1 GB RAM each.

4 Computational results

Figure 7 illustrates the simulated behaviour of the closed-cell cellular structure under compressive and tensile impact loading with different initial pore pressures at a strain rate of 100 s^{-1}. The dotted line represents the tensile failure observed during experimental testing of a cellular structure with relative density of 0.7 and without considering the pore pressure under quasi-static loading conditions [11]. Under compressive loading the pore volume decreases and consequently the internal pore pressure increases, see Figure 8. This mechanism leads to increase of the homogenised yield stress (e.g. increase of 10.6 % for considered example, Figure 8), since the pressure inside the pore acts in the opposite direction than the external loading. With higher pore pressure the cellular structure exhibits higher stress levels during the plastic deformation and thus absorbs more impact energy, Figure 8. Furthermore, higher pore pressure contributes to delayed and slower densification of the cellular structure, i.e. the inflection point occurs at a higher strain, see Figure 7.
During tensile loading the higher pore pressure lowers the homogenised yield stress (e.g. decrease of 18.7 % for considered example, Figure 9). With higher pore pressure the cellular structure exhibits lower stress levels during the plastic deformation and thus absorbs less impact energy, Figure 9.
A higher effect of the internal pore pressure would be observed at lower relative densities.

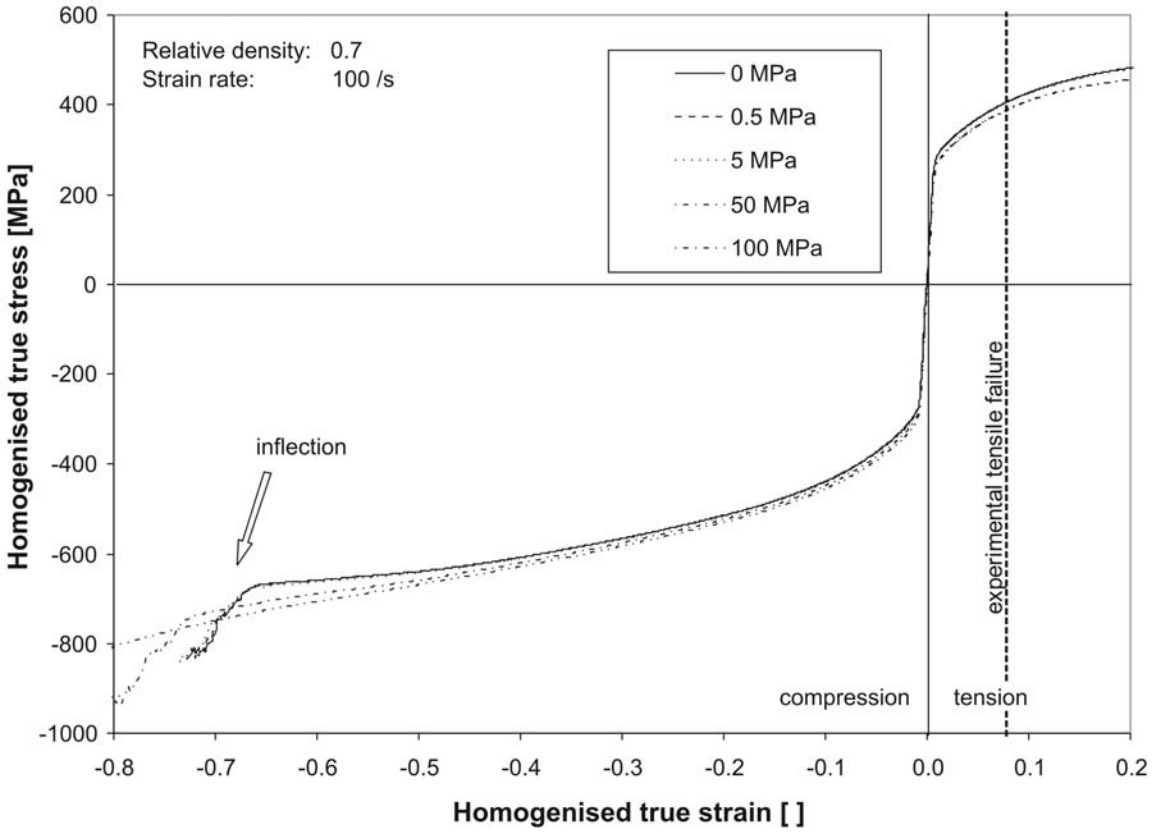

Figure 7: Response of closed-cell cellular structure with initial pore pressure to impact loading

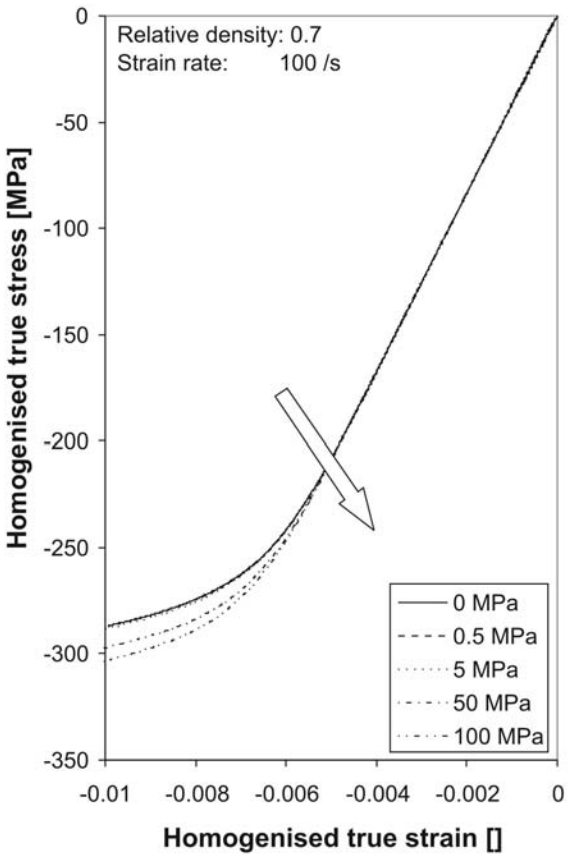

Figure 8: Compressive loading

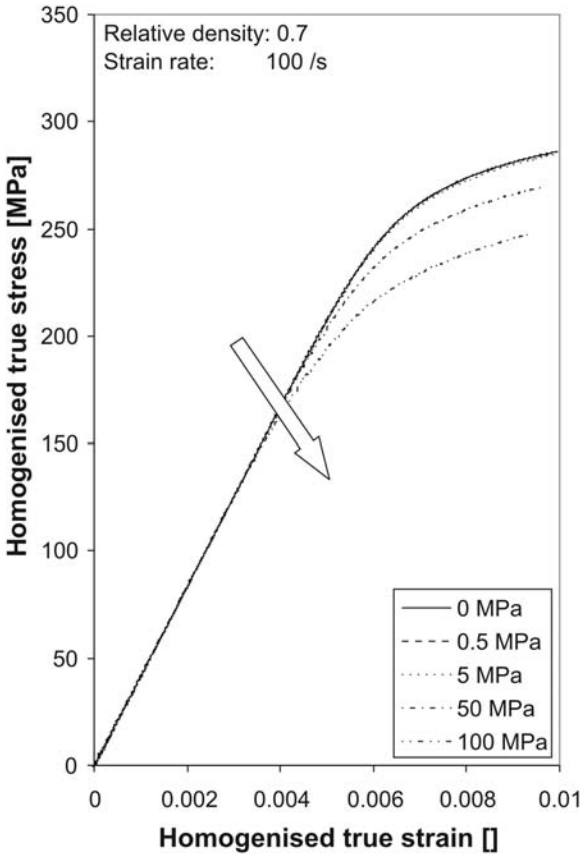

Figure 9: Tensile loading

Figures 10 and 11 illustrate the difference between cell deformation at higher and lower initial pore pressure. As expected, the pore compresses more in the case of lower initial pore pressure than in the case of higher pore pressure. High pore pressure also results in higher base material deformation (Figures 10 and 11).

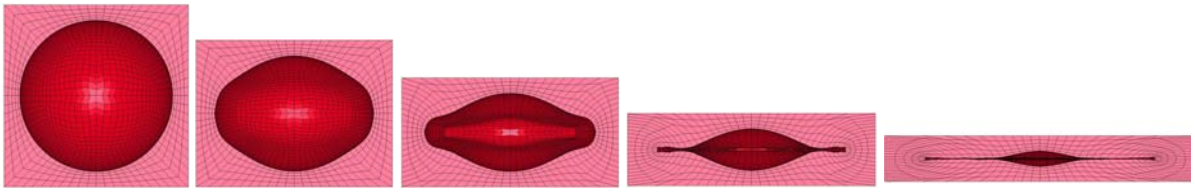

Figure 10: Cell deformation under compressive loading with initial pore pressure 0.5 MPa

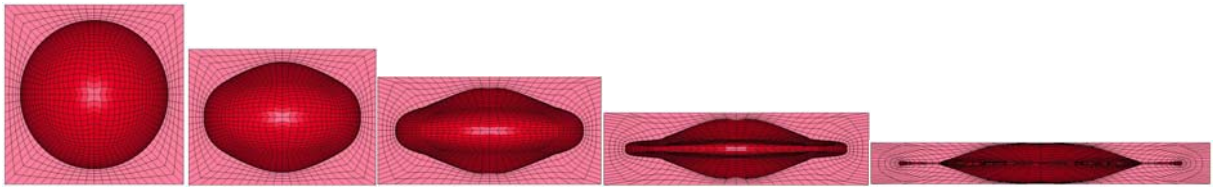

Figure 11: Cell deformation under compressive loading with initial pore pressure 100 MPa

5 Conclusion

The initial results have proven that the influence of the gas inside the cells in closed-cell structures influences the homogenized yield stress and might be even more important at lower relative densities. However it is worth noting that the pore gas pressure influence changes regarding the loading type, i.e. has positive effects under compressive loading and negative under tensile loading. The closed-cell structures, with gas trapped inside the cells under high deformation, can lead to very high internal pore pressure which results in increase of overall material stiffness during the deformation process and higher energy absorption.
The new constitutive laws accounting different relative densities, base materials, pore gases, strain rates and pore pressures will be derived with the described numerical model (Figure 13). Those models will be easy and economical to use in any finite element software.

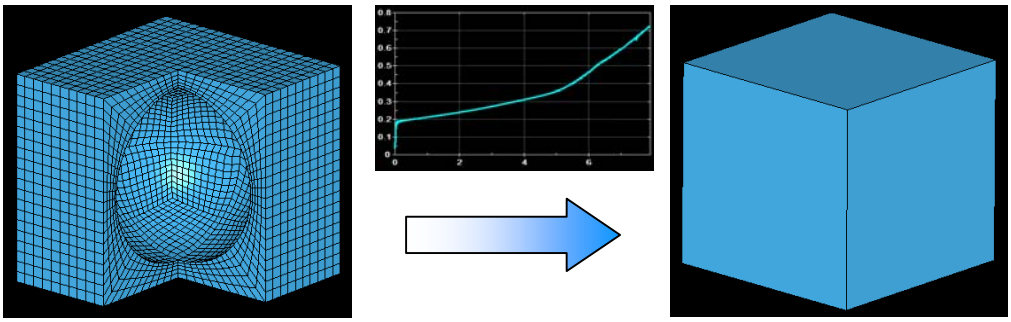

Figure 13: Constitutive model for closed-cell structures

Future research work will be focused on experimental testing and also detailed study of fluid filler influences on mechanical behavior of open-cell cellular materials, taking into account different filler fluids and strain rates with application oriented towards the optimal energy absorption.

References

[1] Altenhof, A, Ames, W, (2002), “Strain rate effects for aluminum and magnesium alloys in finite element simulations of steering wheel impact test”, Fatigue Fract. Engng. Mater. Struct. 25, Blackwell Sci. Ltd.
[2] Ashby, MF, Evans AG, Fleck, NA, Gibson, LS, Hutchinson, JW, Wadley, HNG, (2000), “Metal foams: a design rule”, Boston, Butterworth-Heinemann.
[3] Banhart, John, (2001), “Manufacture, characterisation and application of cellular metals and metallic foams”, Progress in Materials Science 46, Elsevier Science Ltd.
[4] Bodener, SR, Symonds, PS, (1962) “ Experimental and theoretical investigation of the plastic deformation of cantilever beam subjected to impulse loading”, J. Appl. Mech. 29.
[5] Deshpande, VS, Fleck, NA, (2000), “Isotropic constitutive models for metallic foams”, Journal of the Mechanics and Physics of Solids 48, Elsevier Science Ltd.
[6] Elzey, DM, Wadley, HNG, (2001), “The Limits of Solid State Foaming”, Acta Materialia 94, Elsevier Science Ltd.
[7] Gibson, LJ, Ashby, MF, (1997), “Cellular solids: structure and properties”, Cambridge University Press.
[8] Hallquist, John, (1998), “Theoretical manual”, Livermore Software Technology Corporation.
[9] Hallquist John, (2003), “Keyword manual”, Livermore Software Technology Corporation.
[10] Lankford, J, Dannemann, KA, (1998), “Strain Rate Effects in Porous Materials”, Mat. Res. Soc. Symp. Proc. Vol. 521.
[11] Öchsner, Andreas, (2003), “Experimentelle und numerische Untersuchung des elasto-plastischen Verhaltens zellularer Modellwerkstoffe”, Düsseldorf, VDI Verlag GmbH.
[12] Öchsner, Andreas, Mishuris, Gennady, Gracio, Jose, (2004), “Modelling of the multiaxial elasto-plastic behaviour of porous metals with internal gas pressure”, Elsevier Science Ltd.
[13] Ohrndorf, A, Schmidt, Krupp, U, Christ, HJ, (2000), „Mechanische Untersuchung eines geschlossenporigen Aluminiumschaums“, Deutscher Verband für Materialforschung und –prüfung e.V., Bad Nauheim.

